nature portfolio

Peer Review File

Reconfigurable Terahertz Optoelectronic Logic through Charge-Density-Wave Phase Engineering

Corresponding Author: Dr Libo Zhang

This file contains all reviewer reports in order by version, followed by all author rebuttals in order by version.

Version 0:

Reviewer comments:

Reviewer #1

(Remarks to the Author)
The manuscript 'Phase-Transition-Driven Reconfigurable Thermoelectric Logic in Correlated Electron Systems' Sun et al. shows terahertz (THz) photodetector with two dimensional TaS2. The TaS2 photodetector can detect THz illumination with high photoresonsivity by the CDW phase transition. Reconfigurable memory and logic operations are implemented using THz photodetectors via CDW. There are previous studies on THz research utilizing the CDW characteristics of TaS2, and the application seems to be the main novelty of the manuscript. However, the content and explanation on the reconfigurable photoelectric logic characteristic is insufficient. It seems difficult to meet the high standard of Nature communications. Below are some comments.
1. What is the THz frequency of the light source used in Figure 1f? An explanation is needed regarding the reason for the hysteresis. What is the meaning of the arrows in the figure?
2. In figure 2d, what is the bias voltage?
3. Figure 2a shows the device schematics. How about device schematics for figure 1 c, d, f? Is it the same or not?
4. In figure 3c, the difference of threshold voltage is quite small. In my opinion, it is difficult to distinguish B and C, E and F
6. It is hard to understand the meaning of truth table in figure 3d. There is not any information about Vds, Last, Out
7. In the manuscript, authors used 'NC-CDW', 'IC-CDW'. But in the figure authors used 'N-CDW', 'I-CDW'. There is a possibility of confusion due to the use of different abbreviations for the same terms. It seems necessary to use consistent abbreviations throughout.

Reviewer #2

(Remarks to the Author)
The authors present a reconfigurable logic system based on CDW-driven phase transitions in TaS2, tailored for terahertz optoelectronic applications. They demonstrate that thermal, electrical, and optical stimuli can effectively modulate the phase of TaS2, enabling deterministic switching between resistive and dissipation-less states. Additionally, the device exhibits a responsivity of 6.79 A/W, a NEP of 2.64×10-9 W/Hz1/2, and an ultra-fast response time of 2.5 μs at 0.3 THz. Furthermore, they applied this system to Secure Multicolor Recognition. While the manuscript reports compelling results, there remain critical questions that must be addressed to thoroughly evaluate the potential and limitations of this approach.

1- Are the results presented in Figure 2b derived from DFT calculations performed by the authors, or are they sourced from previous papers? If the DFT results are original to this study, please provide a comprehensive explanation of them. If they are taken from prior work, kindly cite the appropriate references.
2- Figure 2g presents results for biases ranging from 0 to 700 mV. What is the rationale behind selecting this specific voltage range? Does an irreversible phase change occur at higher biases? It would be helpful if the authors could provide a detailed explanation regarding this choice.
3- The explanation regarding Figure S4 (THz imaging) is incomplete. To enhance the clarity of the manuscript, I recommend providing a comprehensive explanation of this figure.
4- In Figure 3, the authors have demonstrated different logic states using various bias voltage and THz wave intensities as inputs. However, there are two key concerns:
i) In the tables presented in Figure 3d, one of the parameters is labeled as "last", but no explanation is provided for this parameter. What does "last" represent, and what is its physical significance?

ii) Are basic logic circuits, such as AND/OR and NAND/NOR gates, achievable with this structure? If not, it may be challenging to accurately describe this system as a "reconfigurable logic system". The authors should address this issue and provide further experiments.
5- TaS2 is a vdW material, and in such materials, the electronic properties can vary significantly depending on their thickness. Therefore, analyzing the thickness of this material using AFM appears essential. Could variations in thickness, either smaller or larger, affect its CDW properties? Investigating this aspect would enhance the comprehensiveness of the research.
6- In Figure 1e, both the applied voltage and THz waves can influence the "device temperature" in addition to affecting the electromagnetic properties and electric field. As a result, the parameters of temperature, bias, and wave intensity are not entirely independent. The authors should consider this interdependence when presenting this figure and provide an explanation to address this issue.
7- In explanation of figure 3, the authors mention LRS and HRS modes, but the magnitude of the difference (switching) between them is not provided. Since this switching is a critical parameter for evaluating the performance of the system, it is important to clarify whether there is a significant difference between the LRS and HRS modes. I recommend that the authors include a detailed explanation of this aspect.

Reviewer #3

(Remarks to the Author)
This paper presents 1T-TaS_2 as a promising material for tunable thermoelectric and reconfigurable logic applications, leveraging its distinct charge-density wave (CDW) phases. By employing electric and terahertz (THz) pulse stimuli, the authors demonstrate its potential for efficient, low-latency, in-memory optoelectronic device applications. The study highlights that the various CDW states of 1T-TaS_2 are highly responsive to THz radiation across different frequencies and bias voltages, enabling the realization of a reconfigurable logic device. The device operates by treating both the bias voltage and the THz input as inputs for logical functionality. Furthermore, the authors explore recognition and encrypted communication capabilities by utilizing the reconfigurable logic function under varying light intensities and bias voltage conditions. Followings are the comments for the manuscript prior to publications.

Comment:
1. Caption Fig. 1e, f is not correct (shuffled).
2. The representation of N-CDW and I-CDW in Fig1 (d) is misleading.
3. Nomenclature for LRS for NC-CDW phase and HRS for I-CDW phase inconsistent with their actual resistivity response in 1T-TaS2.
4. What is the correlation between T_fall and T_rise with incident optical powers? How much remanence Iph value after T_fall. There is asymmetry in T_fall for first 50% decrease in Iph value to remaining 50%. Why is this happening so?
5. Are there any frequency dependencies for photocurrent signal under different incident optical powers?
6. In caption of Fig. 2d “incident” appears two times.
7. Why is the current responsivity under different bias voltages within the range of 0.24 THz to 0.3 THz? Is it related to the wavelength of CDW instability?
8. Are the changes induced from application of electric bias or incident THz pulses are reversible especially in the view of CDW instabilities? The validation of the truth table (Fig.3) should also be checked in multiple cycles and with a slight temperature change.
9. What is the optimal thickness of TaS2 for which it shows best THz optoelectronic sensing and reconfigurable logic computation? How does it vary with thickness?
10. What is the role of hBN-TaS2 interface for propagation of CDW-transport properties especially in the vicinity of THz perturbing stimuli?

Version 1:

Reviewer comments:

Reviewer #1

(Remarks to the Author)
The authors have addressed all of my questions in their response. The manuscript now presents the results more clearly. If the novelty of this research is acknowledged by the other reviewers, I believe it would be appropriate for publication in Nature Communications.

Reviewer #2

(Remarks to the Author)
About question #1:
- You mention that the response saturates beyond 0.25 V/um (0.7 V) and that higher voltages could induce irreversible changes or material damage. Could the authors clarify whether any hysteresis or degradation was observed when briefly exceeding this threshold during preliminary tests?

- Is there experimental evidence (e.g., Raman, electrical cycling tests) confirming that operation within the 0-700 mV range avoids any cumulative structural or phase damage over repeated measurements?

About question #7:
- The reported resistance contrast between LRS (500 Ω) and HRS (200 Ω) results in a relatively modest switching ratio. Could the authors comment on whether this level of contrast is sufficient for robust logic operation, especially under noisy or low-signal conditions?

Reviewer #3

(Remarks to the Author)
I am satisfied with the point by point response from the authors. The revised manuscript can be published with no further revision from my side.

Version 2:

Reviewer comments:

Reviewer #2

(Remarks to the Author)
The authors have satisfactorily addressed my concerns, and the manuscript now presents the results more clearly. Assuming the novelty of this research is acknowledged by the other reviewers, I support its publication in Nature Communications.

Dear Editor,

We acknowledge both the Editor and the reviewers for their constructive comments and kind suggestions, which helped us in a careful improvement of the scientific quality of the manuscript, as well as its readability (including style). Reviewers' reports are valuable and served as important guides to our research. Following the reviewers' comments, we have carefully **revised the manuscript and the supplementary material** with elaborate discussions and additional experimental data. Here, we submit the revised version of our paper for your consideration.

All changes in the revised manuscript are highlighted in red.

———— REPLY TO REVIEWER 1————

REFEREE:The manuscript 'Phase-Transition-Driven Reconfigurable Thermoelectric Logic in Correlated Electron Systems'Sun et al. shows terahertz (THz) photodetector with two dimensional TaS_2. The TaS_2 photodetector can detect THz illumination with high photoresonsivity by the CDW phase transition. Reconfigurable memory and logic operations are implemented using THz photodetectors via CDW. There are previous studies on THz research utilizing the CDW characteristics of TaS2, and the application seems to be the main novelty of the manuscript. However, the content and explanation on the reconfigurable photoelectric logic characteristic is insufficient. It seems difficult to meet the high standard of Nature communications.

AUTHORS' REPLY: We are deeply grateful for your thorough evaluation and constructive feedback on our manuscript titled " Reconfigurable Terahertz Optoelectronic Logic through Charge-Density-Wave Phase Engineering". Your insights have been invaluable in guiding the improvements we have made to address the concerns raised, particularly regarding the detailed explanation and demonstration of terahertz mechanism、reconfigurable photoelectric logic characteristics.

In addressing your comments, we have delved deeper into the underlying mechanisms and demonstrated unprecedented performance enhancements that set our work apart from prior studies. While Wu et al. pioneered the use of charge-density-wave (CDW) properties in TaS_2 for THz detection (Wu et al., Sci. Adv. 2018;4:eaao3057), our study introduces novel insights into the phase-transition dynamics and establishes a direct correlation between CDW mode excitation and ultrafast photodetection, thereby advancing the field toward practical ultra-broadband applications. We have meticulously elucidated the direct coupling between terahertz radiation and CDW collective modes, revealing intricate mechanisms of coherent lattice distortion and electronic transport modulation. This stands in contrast to previous approaches that often treated these interactions as black-box phenomena, providing unprecedented insights into quantum state manipulation. Our work introduces a novel mechanism for reconfigurable logic and memory operations in TaS_2-based THz photodetectors, rooted in the dynamic manipulation of CDW phase transitions under multi-field stimuli. Unlike prior studies (*Wu et al., Sci. Adv. 2018;4:eaao3057*), which focused on electric field-driven CDW modulation for photodetection, our approach leverages temperature gradients, THz excitations, and bias to achieve precise control over the electronic phase landscape. The device exhibits exceptional performance characteristics that distinguish it from current state-of-the-art THz detectors[1-12]. With a current responsivity of 5.49 A/W and an ultrafast response time of 1.7 μs, our system outperforms conventional detectors limited by thermal detection mechanisms.

Importantly, the study represents a significant advancement in the field of terahertz optoelectronic intelligent sensing, with breakthroughs being made in two major innovative directions: 1) Reconfigurable Optoelectronic Logic. Whilst infrared detector-based optoelectronic hybrid logic units exhibit fast response characteristics, their complex architecture involving multi-electrode manipulation and intrinsic infrared absorption loss hinders efficient unit reconfiguration [13-16]. Our study proposes a real-time programmable logic operations (AND/OR) based on terahertz radiation intensity thresholds, extending the dynamic response range of the device in the 0.24-0.3 THz band. This innovation exploits the bias regulation mechanism of the CDW phase transition process. 2) Secure Multicolor Recognition and Encrypted Communication. Existing image encryption and recognition within sensors are mostly limited to monochrome/grayscale images, lacking efficient discrimination of multiple colours [17-18]. This device provides a novel physical layer encryption solution for next-generation wireless communication systems by establishing a terahertz intensity-logical state-colour space mapping relationship to enable information transmission with independent secret keys.

Correspondingly, we modify the manuscript point by point based on these suggestions. Our revised manuscript now includes additional experimental data and enhanced explanations.

Material	Frequency	Responsivity	Response time	Refs.
TaS_2	0.3 THz	5.49 A/W (>700 V/W)	1.7 μs	This work
TaS_2	0.12 THz	9.39 A/W (>1300 V/W)		This work
CNT-Gra	0.11 THz	24.6 mA/W	12.6 μs	1
TaNiSe	~0.265 THz	1350 A/W	550 ns	2
PtTe	0.12 THz	1.6 A/W	17 μs	3
Gra-Ta_2NiSe	0.3 THz	18.2 mA/W	720 ns	4
Gra-Ta_2NiSe	0.12 THz	24.2 mA/W		
ZrGeSe	0.26 THz	0.11 A/W	8.3 μs	5
HgTe	0.3 THz	0.04 A/W	3 μs	6
Graphene	1.8-4.2 THz	20 V/W	30 ns	7
Graphene	0.15 THz	400 V/W	20 μs	8
Graphene	3 THz	-	3.3 ns	9
Black phosphorus	0.3 THzTHz	0.15 V/W	-	10
Black phosphorus	0.29 THz	1.5 V/W	15 μs	11
T_d-$MoTe_2$	2.52 THz	0.53 mA/W	26 μs	12

Reference

1. Ma, W. et al. Detection of Long Wavelength Photons via Quasi-Two-Dimensional Ternary Ta 2 NiSe 5. ACS Appl. Electron. Mater. 4, 2979–2986 (2022).

2. He, Y. et al. Carbon-based self-powered terahertz detector with multi-walled carbon nanotubes-graphene heterostructure. Carbon 221, 118886 (2024).

3. Xu, H. et al. PtTe 2 -Based Type-II Dirac Semimetal and Its van der Waals Heterostructure for Sensitive Room Temperature Terahertz Photodetection. Small 15, 1903362 (2019).

4. Zhang, K. et al. Self-driven and ultrasensitive room-temperature terahertz photodetector based on graphene-Ta2NiSe5 van der Waals heterojunction. Infrared Physics & Technology 128, 104474 (2023).

5. Zuo, X. et al. High sensitivity HgTe room temperature terahertz photodetector. APL Photonics 8, 046109 (2023).

6. Zhang, L. et al. Ultrasensitive and Self-Powered Terahertz Detection Driven by Nodal-Line Dirac Fermions and Van der Waals Architecture. Advanced Science 8, 2102088 (2021).

7. Castilla, S., et al. Fast and sensitive terahertz detection using an antenna-integrated graphene pn junction. Nano Lett. 19, 2765-2773 (2019).

8. Viti, L., Purdie, D. G., Lombardo, A., Ferrari, A. C., Vitiello, M. S. HBN encapsulated, graphene-based, room-temperature terahertz receivers, with high speed and low noise. Nano Lett. 20, 3169-3177 (2020).

9. Amirmazlaghani, M., Raissi, F. Feasibility of room-temperature GHz-THz direct detection in graphene through hot-carrier effect. Ieee T Device Mat Re 18, 429-437 (2018).

10. Viti, L., et al. Black phosphorus terahertz photodetectors. Adv. Mater. 27, 5567- 5572 (2015).

11. Guo, W. L., et al. Sensitive terahertz detection and imaging driven by the photothermoelectric effect in ultrashort-channel black phosphorus devices. Adv. Sci. 7, 1902699 (2020).

12. Yang, Q., et al. A Centimeter-Scale Type-II Weyl Semimetal for Flexible and Fast Ultra-Broadband Photodetection from Ultraviolet to Sub-Millimeter Wave Regime. Adv. Sci. 10, 2205609 (2023).

13. Liu, C. et al. Small footprint transistor architecture for photoswitching logic and in situ memory. Nat. Nanotechnol. 14, 662–667 (2019).

14. Chen, H. et al. Logic gates based on neuristors made from two-dimensional materials. Nat Electron 4, 399–404 (2021).

15. Wu, Y. et al. Dynamic upconversion multicolour editing enabled by molecule-assisted opto-electrochemical modulation. Nat. Commun 12, 2022 (2021).

16. Yu, S. E. et al. J-MISFET Hybrid Dual-Gate Switching Device for Multifunctional Optoelectronic Logic Gate Applications. ACS Nano 18, 11404–11415 (2024).

17. Shao, B. et al. Highly Trustworthy In-Sensor Cryptography for Image Encryption and Authentication. ACS Nano 17, 10291–10299 (2023).

18. Dodda, A. et al. All-in-one, bio-inspired, and low-power crypto engines for near-sensor security based on two-dimensional memtransistors. Nat. Commun 13, 3587 (2022).

REFEREE: 1) What is the THz frequency of the light source used in Figure 1f? An explanation is needed regarding the reason for the hysteresis. What is the meaning of the arrows in the figure?

AUTHORS' REPLY: We thank the referee for the insightful comments. Below, we address each point raised in the comment.

1. THz Frequency of the Light Source: The terahertz light source used in Figure 1f (now Figure 2b in the revised manuscript) operates at a frequency of 0.12 THz. This frequency was chosen to effectively couple with the lattice dynamics of 1T-TaS_2, which induces coherent vibrations of Ta atoms, modulating the Ta-Ta bond distances and perturbing the periodic lattice distortion associated with the CDW.
2. Explanation of Hysteresis: The hysteresis can be attributed to the following mechanisms: (1) Field-Induced Depinning and Joule Heating: As reported in prior studies[1-3], the electric-field-driven phase transition in 1T-TaS_2 results from a combination of field-induced depinning of the CDW and Joule heating effects. The applied electric field overcomes the pinning potential, allowing the CDW to slide, while Joule heating ($P=I^2R$) raises the local temperature, further facilitating the transition to the IC-CDW state. (2) THz-Induced Lattice Dynamics: The 0.12 THz field induces coherent vibrations of Ta atoms, modulating the Ta-Ta bond distances and perturbing the periodic lattice distortion associated with the CDW. This reduces the pinning potential, promoting localized CDW sliding or collapse, which manifests as a stepwise decrease in resistance. This THz-driven effect synergistically enhances the nonlinear response of the current to the applied bias, with the maximum amplification occurring near the threshold voltage V_{th-H}. During the reverse sweep, the recovery of the pinning potential and the cooling of the

device lag behind, resulting in a lower V_{th-L}, thus contributing to the hysteresis.

3. Meaning of the Arrows in the Figure: The forward arrow (increasing voltage) corresponds to the sweep from minimun to the maximum voltage, during which the threshold switching occurs at V_{th-H}. The reverse arrow (decreasing voltage) indicates the sweep back to 0 V, where the reverse transition occurs at V_{th-L}.

To address potential ambiguity, we have revised the figure by adding a clearer annotation of the sweep directions and the definitions in Figure 2b. Correspondingly, we have updated the main text by adding a detailed explanation in lines 224-226 on Page 8-9 and lines 237-256 on Page 9-10 of the revised manuscript.

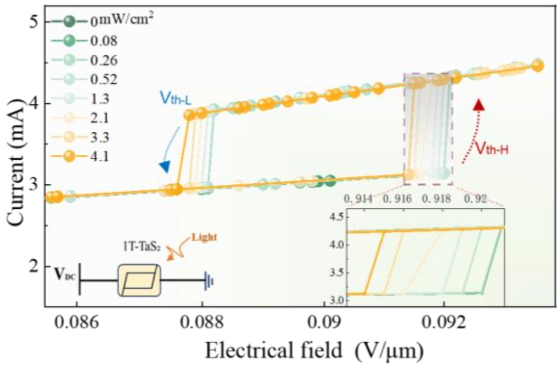

Revised Figure R1 (**Fig. 2b in the revised manuscript**) Current-voltage characteristics of the device under varying THz illumination intensities (0-4.1 mW/cm²), showing distinct hysteresis loops and threshold voltage shifts. Inset: equivalent circuit diagram and magnified view of threshold voltage region.

Reference

1.M. Yoshida, T. Gokuden, R. Suzuki, M. Nakano, Y. Iwasa, Current switching of electronic structures in two-dimensional 1T−TaS2 crystals. Physical Review B 95, 121405 (2017).

2.G. Grüner, The dynamics of charge-density waves. Reviews of Modern Physics 60, 1129-1181 (1988).

3.M. Yoshida, R. Suzuki, Y. Zhang, M. Nakano, Y. Iwasa, Memristive phase switching in two-dimensional 1T-TaS_2 crystals. Science Advances 1, e1500606 (2015).

REFEREE: 2) In figure 2d, what is the bias voltage?

AUTHORS' REPLY: 2) Our sincere thanks go to the reviewer for taking the time to review our work and for their thoughtful comments and recommendations.As shown in supplementary material Figure S3, we selected the position with the highest response as the electric field intensity, which is approximately 0.092 V/μm. In order to present the information more logically, we have revised the format of Figure 2d and repositioned it as Figure 2c in the revised manuscript and added appiled electrical field of 0.092 V/μm on page 10, line 253. We believe these modifications not only address the reviewer's specific inquiry but also significantly enhance the scientific rigor and communicative precision of our manuscript.

REFEREE: 3) Figure 2a shows the device schematics. How about device schematics for figure 1 c, d, f? Is it the same or not?

AUTHORS' REPLY: 3) We appreciate the referee's question regarding the consistency of device schematics. The device structures depicted in Figures 1c, 1d, and 1f are identical to that shown in Figure 2a. All measurements were conducted using the same TaS_2-h-BN integrated device configuration, which consists of a 1T-TaS_2 thin film capped with h-BN for oxidation protection. This uniformity ensures that the observed electrical characteristics and phase transition behaviors are directly comparable across the different experimental conditions presented in these figures. To prevent any potential misinterpretation by readers regarding the device structure, we have added a microscopic image of the device in Figure 1e in the revised manuscript.

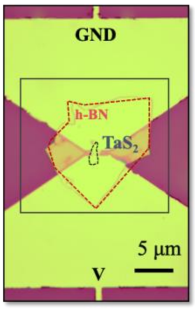

Revised Figure R2(Fig. 1e in the revised manuscript) Optical image of a two-probe 1T-TaS_2 device. One electrode is grounded (GND) and the other was used to apply the voltage (V).

REFEREE: 4) In figure 3c, the difference of threshold voltage is quite small. In my opinion, it is difficult to distinguish B and C, E and F

AUTHORS' REPLY: 4) We are profoundly grateful for the reviewer's discerning eye, which has allowed us to provide deeper insights into our experimental methodology and results. The definition of state B is 1.72 V to 1.74 V, and for state C, 1.74 V to 1.76 V, with a 20 mV gap between the threshold voltages. The voltage levels for states E and F are defined as 1.95 V to 1.97 V and 1.97 V to 1.99 V, respectively, and both of these can be precisely controlled by the voltage input source. In previous studies, the threshold switching behaviour of logic circuit components has only varied by 10-100 mV[1-3], mainly to reduce dynamic and static power consumption and increase the speed of device switching states while achieving device-specific memory functions. The primary text explores the optical power of varying intensities and demonstrates that enhancing the optical power can elevate the threshold voltage. However, the central study focuses on the physical mechanism in low light conditions, resulting in a relatively modest increase in threshold voltage. In the context of small-scale integrated circuits, a digital-to-analogue converter (DAC) is typically employed to supply voltage to components. A 12-bit DAC, for instance, is capable of achieving a voltage resolution of 1.22 mV at a reference voltage of 5 V. Consequently, achieving a voltage resolution with a precision of 20 mV is more feasible [4, 5].

Reference

1 Fiori, G., Bonaccorso, F., et al. Two-dimensional materials for next-generation computing technologies. Nature Nanotechnology, 15(12), 987-993, (2020).

2 Hu, J., Li, H., et al. All-2D-Materials Subthreshold-Free Field-Effect Transistor with Near-Ideal Switching Slope. ACS Nano, 18(5), 12345-12356, (2024).

3 Cheng, R. et al. Toward Learning in Neuromorphic Circuits Based on Quantum Phase Slip Junctions. Front. Neurosci. 15, 765883, (2021).

4 R. J. Baker, CMOS: Circuit Design, Layout, and Simulation, 3rd ed., Wiley-IEEE Press, 2010.

5 B. Razavi, Design of Analog CMOS Integrated Circuits, 2nd ed., McGraw-Hill Education, 2016.

REFEREE: 5) It is hard to understand the meaning of truth table in figure 3d. There is not any information about Vds, Last, Out

AUTHORS' REPLY: We sincerely appreciate the reviewer pointing out this lack of clarity in Figure 3d. We have now provided comprehensive explanations for all parameters in the truth tables to ensure better understanding: "V_{ds}" represents the bias voltage applied to the device, where $V_{ds} = 0$ corresponds to lower voltage points (C, D, or B depending on which table) and $V_{ds} = 1$ corresponds to higher voltage points (F or E) on the I-V curves in Figure 3c. "Last" indicates the initial resistance state of the device before the current operation: 0 represents the high resistance state (HRS, corresponding to NC-CDW phase) and 1 represents the low resistance state (LRS, corresponding to IC-CDW phase). This parameter captures the device's state-dependent behavior resulting from the hysteresis shown in Figure 3c. Finally, "Out" denotes the resulting based on the reconfigurable logic operations as illustrated in the circuit diagrams in Figure 3e.

To address this issue, we have added detailed explanations of these parameters in the revised manuscript (lines 412-415 at page 15-16) and have also included clearer labeling in the figure caption.

REFEREE: 6) In the manuscript, authors used ‘NC-CDW’, ‘IC-CDW’. But in the figure authors used ‘N-CDW’, ‘I-CDW’. There is a possibility of confusion due to the use of different abbreviations for the same terms. It seems necessary to use consistent abbreviations throughout.

AUTHORS’ REPLY: 6) We thank the reviewer for raising the issue of inconsistent abbreviations in our manuscript. We have made modifications in the text and figures to unify the abbreviations of nominal concepts (‘NC-CDW’, ‘IC-CDW’).

———— REPLY TO REVIEWER 2————

REFEREE: The authors present a reconfigurable logic system based on CDW-driven phase transitions in TaS_2, tailored for terahertz optoelectronic applications. They demonstrate that thermal, electrical, and optical stimuli can effectively modulate the phase of TaS_2, enabling deterministic switching between resistive and dissipation-less states. Additionally, the device exhibits a responsivity of 6.79 A/W, a NEP of 2.64×10-9 W/Hz$^{1/2}$, and an ultra-fast response time of 2.5 μs at 0.3 THz. Furthermore, they applied this system to Secure Multicolor Recognition. While the manuscript reports compelling results, there remain critical questions that must be addressed to thoroughly evaluate the potential and limitations of this approach.

AUTHORS' REPLY: We sincerely thank the reviewer for having appreciated our work. We also thank the reviewer for the constructive comments and suggestions, which have helped us to further improve the quality of the manuscript. All referee's comments and suggestions were carefully addressed at the best of our possibilities. Correspondingly, we revised the text of the manuscript in order to incorporate modifications to address referee's comments.

REFEREE: 1) Are the results presented in Figure 2b derived from DFT calculations performed by the authors, or are they sourced from previous papers? If the DFT results are original to this study, please provide a comprehensive explanation of them. If they are taken from prior work, kindly cite the appropriate references.

AUTHORS' REPLY: 1) Thank you for your valuable feedback. According to the reviewer's suggestion, we added a reference to this panel.

REFEREE: 2) Figure 2g presents results for biases ranging from 0 to 700 mV. What is the rationale behind selecting this specific voltage range? Does an irreversible phase change occur at higher biases? It would be helpful if the authors could provide a detailed explanation regarding this choice.

AUTHORS' REPLY: 2) We are grateful to the reviewer for their insightful questions and valuable suggestions. The voltage range (0–700 mV) was selected based on current-voltage measurements identifying a critical threshold at 0.23 V/μm (650 mV), where the NC-CDW to IC-CDW phase transition triggers a sharp response increase. Beyond 0.25 V/μm (0.7 V), the response saturates, meeting our performance goals while avoiding excessive current densities that could induce irreversible CDW state changes or material damage. This range balances optimal functionality with device stability and reproducibility.

REFEREE: 3) The explanation regarding Figure S4 (THz imaging) is incomplete. To enhance the clarity of the manuscript, I recommend providing a comprehensive explanation of this figure.

AUTHORS' REPLY: 3) We thank the reviewer for highlighting the need for a more detailed explanation of Figure S4. We have comprehensively detailed the description of the THz imaging setup and results in the revised Supporting Information. Figure S4 demonstrates our device's capability for room-temperature THz imaging applications. The left panel illustrates the complete scanning imaging optical path configuration. Our setup employs a confocal arrangement where THz radiation (0.12 THz) from the source is guided through a series of optical components including collimating mirrors, focusing elements. The specimen is positioned at the focal plane of the optical system, and the transmitted THz radiation is collected and directed to our TaS_2-based detector. The right panel presents comparative imaging results of a metal pin: the optical image (right side) alongside its corresponding THz transmission image (left side, shown in false color where red indicates high transmission and blue indicates low transmission). The THz image clearly delineates the metallic structure of the pin, demonstrating the spatial resolution capabilities of our system even at room temperature. This represents a significant advantage over conventional THz detectors that typically require cryogenic cooling for imaging applications. The spatial resolution achieved in this demonstration is approximately 1.5 mm, primarily limited by the wavelength of the 0.12 THz radiation rather than detector sensitivity. The integration time for each pixel was 50 ms, allowing for reasonable image acquisition speeds while maintaining good signal-to-noise ratio.

We have added this comprehensive explanation to the supplementary information section that accompanies Figure S4, providing readers with the technical details necessary to understand both the experimental configuration and the significance of the imaging results.

REFEREE: 4) In Figure 3, the authors have demonstrated different logic states using various biasvoltage and THz wave intensities as inputs. However, there are two key concerns: i) In the tables presented in Figure 3d, one of the parameters is labeled as "last", but no explanation is provided for this parameter. What does "last" represent, and what is its physical significance?

AUTHORS' REPLY: 4) i) We thank the reviewer for this important question regarding the "Last" parameter in Figure 3d. To clarify, "Last" represents the resistance state of the device before the current operation begins. Specifically, Last = 0 indicates that the device is initially in the high resistance state (HRS, corresponding to NC-CDW phase), while Last = 1 indicates that the device is initially in the low resistance state (LRS, corresponding to IC-CDW phase). This parameter is crucial for understanding the hysteretic behavior demonstrated in Figure 3c, where the I-V curves under different THz light intensities (0, 2.1, and 4.1 mW/cm^2) exhibit distinct resistance switching characteristics. The bistable nature of the device allows it to maintain either the HRS or LRS state depending on its previous bias history, which is precisely what the "Last" parameter captures.

For example, in the C→F operation (first table in Figure 3d), when Light density = 00 (no THz radiation), V_{ds} = 0 (corresponding to point C in Fig. 3c), and Last = 0 (device initially in HRS), the output remains 0 (device stays in HRS). This path-dependent behavior forms the basis of our reconfigurable logic operations as illustrated in the circuit diagrams in Figure 3e.

Following the reviewer's suggestion, we have added a clear explanation of this parameter in lines 412-415 on Page 15-16 of the revised manuscript.

ii) Are basic logic circuits, such as AND/OR and NAND/NOR gates, achievable with this structure? If not, it may be challenging to accurately describe this system as a "reconfigurable logic system". The authors should address this issue and provide further experiments.

AUTHORS' REPLY: 4) ii) We thank the reviewer for raising this important point. I apologise for the lack of clarity in the preceding main text, and undertake to improve this aspect in future. In contrast to the majority of infrared spectral memory logic devices, our approach utilised the non-volatile terahertz switching property of the sensor, thereby constructing reconfigurable logic circuit functions, encompassing the fundamental logic circuit element functions. Further details can be found in Figure S10 of the Supplementary Information. The demonstration of the fundamental logic functionality of the device is implemented at varying voltage pulses, including optical/electrical deviations, as well as optical/electrical pulses, allowing for different coding logic and followers to increase the complexity of the functionality. The device integrates terahertz sensitivity, memory retention, and the capacity for reconfiguring logic calculations, thereby achieving an integrated terahertz memory logic functionality. Correspondingly, we have modified the main text by adding lines 347-351 at Page 12.

A

A→C			
Light density	V_{ds}	Last	Out
0	0	0	0
0	1	0	0
0	0	1	0
0	1	1	0
1	0	0	0
1	1	0	0
1	0	1	0
1	1	1	1

B

A→F			
Light density	V_{ds}	Last	Out
0	0	0	0
0	1	0	0
0	0	1	0
0	1	1	1
1	0	0	0
1	1	0	1
1	0	1	0
1	1	1	1

C

A→G			
Light density	V_{ds}	Last	Out
0	0	0	0
0	1	0	1
0	0	1	0
0	1	1	1
1	0	0	0
1	1	0	1
1	0	1	0
1	1	1	1

D

A→D			
Light density	V_{ds}	Last	Out
0	0	0	0
0	1	0	0
0	0	1	0
0	1	1	1
1	0	0	0
1	1	0	0
1	0	1	0
1	1	1	1

E

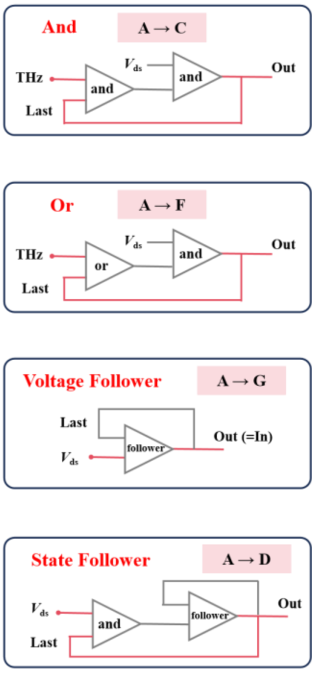

Revised Figure R4(Fig. S6 in the revised manuscript). Demonstration of non-volatile basic optoelectronic logic functions of TaS_2 device. Truth table of the device implementing logic functions at different intensity pulse voltages (light intensity "0" for the dark, "1" for a terahertz wave with a light intensity of 2.1 mW/cm^2 , V_{ds} for the applied bias voltage, and Last and Out for the CDW phase state in which the device is in). (A) And gate; (B) Or gate; (C) Voltage follower; (D) State follower; (E) Schematic diagram of the implemented logic function corresponding to the above figure one by one.

REFEREE: 5) TaS2 is a vdW material, and in such materials, the electronic properties can vary significantly depending on their thickness. Therefore, analyzing the thickness of thismaterial using AFM appears essential. Could variations in thickness, either smaller or larger, affect its CDW properties? Investigating this aspect would enhance the comprehensiveness of the research.

AUTHORS' REPLY: 5) Thanks for your detailed comments and suggestions that have significantly improved the quality of our paper. In response to your suggestion, we have supplemented AFM thickness analysis experiments and further investigated the impact of thickness variations (18 nm, 45 nm, and 107 nm) on the CDW properties of TaS_2. Notably, our I-V measurements reveal that thinner samples require significantly higher electric fields to trigger the phase transition, with the 18 nm sample showing substantially lower conductivity compared to the thicker counterparts. The ordering kinetics of the phase transition were found to become extremely slow as the thickness is reduced, resulting in an emergence of metastable states[1]. The observed thickness dependence likely stems from modifications in the band structure and electron-phonon coupling mechanisms, which are crucial for CDW formation. As dimensionality is reduced, the delicate balance of forces stabilizing the CDW state is progressively altered, requiring stronger external stimuli (higher electric fields) to overcome the modified energy barriers between phases. Our findings align well with previous reports in the literature[2-4].

For a more comprehensive understanding, materials of different thicknesses can exhibit distinct characteristics in I-V testing, with variations observed in the position of the phase transition voltage and the size of the hysteresis window in Figure S7 of the Supplementary Information.

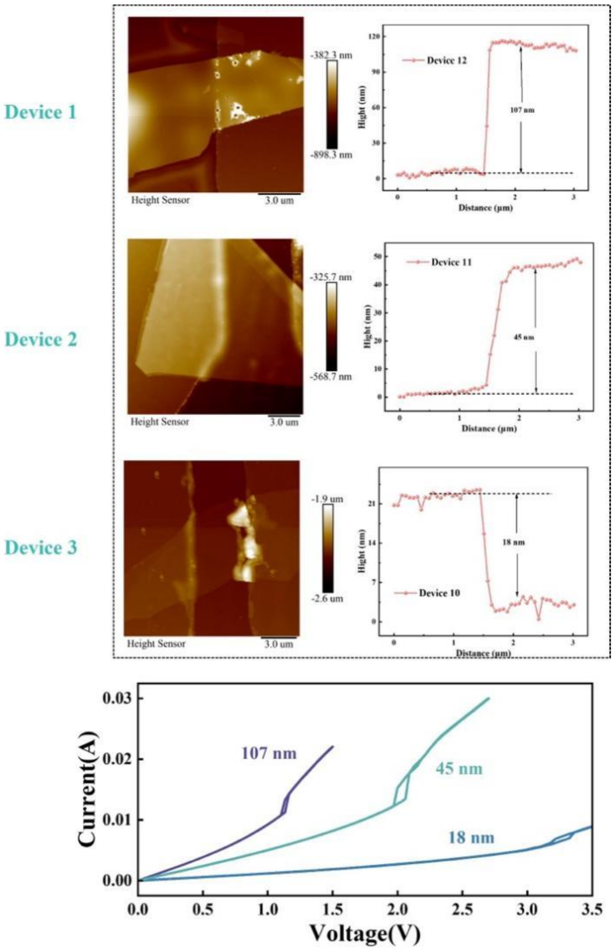

Revised Figure R5(**Fig. S7 in the revised manuscript**). Thickness-dependent I-V characteristics of TaS_2. (A) AFM for there devices of different thickness. (B) Hysteresis I-V characteristics.

Reference

1. M. Yoshida, R. Suzuki, Y. Zhang, M. Nakano, Y. Iwasa, Memristive phase switching in two-dimensional 1T-TaS_2 crystals. Science Advances 1, e1500606 (2015).
2. Y. Yu, F. Yang, X. F. Lu, Y. J. Yan, Y. H. Cho, L. Ma et al., Gate-tunable phase transitions in thin flakes of 1T-TaS_2. Nat Nanotechnol 10, 270-276 (2015).
3. Y. Geng, L. Lei, H. Dong, J. Guo, S. Mi, Y. Li et al., Hysteretic electronic phase transitions in correlated charge density wave state of 1T−TaS_2. Physical Review B 107, (2023).
4. S. Zheng, F. Liu, C. Zhu, Z. Liu, H. J. Fan, Room-temperature electrically driven phase transition of two-dimensional 1T-TaS_2 layers. Nanoscale 9, 2436-2441 (2017).

REFEREE: 6) In Figure 1e, both the applied voltage and THz waves can influence the "device temperature" in addition to affecting the electromagnetic properties and electric field. As a result, the parameters of temperature, bias, and wave intensity are not entirely independent. The authors should consider this interdependence when presenting this figure and provide an explanation to address this issue.

AUTHORS' REPLY: 6) We sincerely appreciate your insightful comment regarding the interdependence of temperature, applied bias, and light intensity in Figure 1e. Thank you for your expert guidance, which brought this critical interdependency to our attention—a factor we had not previously considered in such depth. To address this, we have revised our understanding to distinguish between the environmental temperature (T, the ambient or lattice temperature) and the electronic temperature (T_e, the effective temperature of the electron system), where T_e is modulated by Joule heating from E and hot carrier generation from U, in addition to T. This distinction allows us to better capture the interdependence referee noted, as T_e emerges as a composite parameter that integrates these external influences and directly impacts ΔG. To reflect this in the revised Figure 1e, we propose the following updates: First, we will incorporate T_e as a key parameter, calculated as T_e ~[T, E, U]. Second, we will include an inset schematic within the figure, illustrating the flow of influence: T, E, and U converge to determine T_e, which in turn modulates ΔG, ultimately governing the phase transition between the NC-CDW and IC-CDW states.

Thank you again for your valuable feedback, which has significantly improved the clarity and scientific rigor of our presentation. We have revised the relevant description in the 174-180 line of the 6-7 page of the revised manuscript.

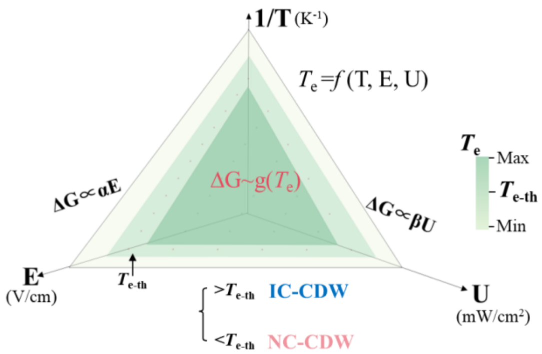

Revised Figure R6 **(Fig. 1e in the revised manuscript)** Triangular diagram illustrating the combined effect of environmental temperature T, electric field E, light intensity U, and phase transition potential barrier (ΔG) on the phase transition of 1T-TaS_2.

REFEREE: 7) In explanation of figure 3, the authors mention LRS and HRS modes, but the magnitude of the difference (switching) between them is not provided. Since this switching is a critical parameter for evaluating the performance of the system, it is important to clarify whetherthere is a significant difference between the LRS and HRS modes. I recommend that the authors include a detailed explanation of this aspect.

AUTHORS' REPLY: 7) We greatly appreciate your thoughtful observation regarding the explanation of Figure 3 and the need to address the magnitude of the resistance switching between the low-resistance state (LRS) and high-resistance state (HRS) modes as controlled by V_{ds} and THz light intensity. In our experiments, the resistance values for these states at room temperatures are approximately 500 Ω for the LRS (IC-CDW) and 200 Ω for the HRS (NC-CDW), yielding a resistance difference of about 300 Ω under the conditions tested.

We have now included these specific resistance values and their ratio in the revised manuscript, along with additional context about how the resistance contrast enables the demonstrated logic operations in lines 380-385 on Page 14-15 of the revised manuscript.

————R E P L Y   T O   R E V I E W E R   3————

REFEREE: This paper presents 1T-TaS_2 as a promising material for tunable thermoelectric and reconfigurable logic applications, leveraging its distinct charge-density wave (CDW) phases. By employing electric and terahertz (THz) pulse stimuli, the authors demonstrate its potential for efficient, low-latency, in-memory optoelectronic device applications. The study highlights that the various CDW states of 1T-TaS_2 are highly responsive to THz radiation across different frequencies and bias voltages, enabling the realization of a reconfigurable logic device. The device operates by treating both the bias voltage and the THz input as inputs for logical functionality. Furthermore, the authors explore recognition and encrypted communication capabilities by utilizing the reconfigurable logic function under varying light intensities and bias voltage conditions. Followings are the comments for the manuscript prior to publications.

AUTHORS' REPLY: We thank the reviewer for carefully reviewing our manuscript, for appreciating our paper and for the constructive comments. We find the suggestions of the referee to be extremely helpful for enhancing the readability of the manuscript. In the following, we address all the comments with a point-by-point reply. Correspondingly, we modify the manuscript based on these suggestions.

REFEREE: 1) Caption Fig. 1e, f is not correct (shuffled).

AUTHORS' REPLY: 1) We sincerely thank you for your thorough review and for identifying the issue with the captions for Figure 1e and Figure 1f, which were inadvertently shuffled in the original manuscript. We apologize for this oversight and appreciate your attention to detail, as it ensures the clarity and accuracy of our presentation.

REFEREE: 2) The representation of NC-CDW and IC-CDW in Fig1 (d) is misleading.

AUTHORS'REPLY: 2) We appreciate the reviewer careful attention and helpful feedback on our manuscript. We have made modifications in the text and images to unify the abbreviations of nominal concepts (NC-CDW phase and IC-CDW phase).

REFEREE: 3) Nomenclature for LRS for NC-CDW phase and HRS for IC-CDW phase inconsistent with their actual resistivity response in 1T-TaS2.

AUTHORS' REPLY: 3) We are thankful to the reviewer for pointing out mistakes and offering useful guidance for improvement. We have corrected the errors in the lines 364-365 at pages 14.

REFEREE: 4) What is the correlation between T_fall and T_rise with incident optical powers? How much remanence Iph value after T_fall. There is asymmetry in T_fall for first 50% decrease in Iph value to remaining 50%. Why is this happening so?

AUTHORS' REPLY: 4) The reviewer questions and suggestions are highly appreciated and will undoubtedly contribute to the enhancement of our research. **(1)** Following the referee's suggestion, we measured the time-resolved photocurrent response at various incident power densities (0.1-2.5 mW/cm²). The rise time ($\tau_{rise} \approx 1.7$ μs) remains remarkably consistent across various incident power densities in Fig. 2i, whereas the fall time (τ_{rall}) exhibits pronounced power dependence, increasing from approximately 3.2 μs at 0.1 mW/cm^2 to 11.6 μs at 2.5 mW/cm^2, revealing the asymmetric dynamics between CDW excitation and relaxation. **(2)** The remanent photocurrent is systematically quantified by analyzing the decay trajectory from 90% to 10% of the peak photocurrent (defining τ_{rall}). **(3)** The power-independent τ_{rise} indicates that the initial phase transformation proceeds via a threshold-activated coherent excitation of CDW collective modes rather than thermal accumulation. The microsecond-scale response substantially outperforms conventional bolometric detectors, confirming direct coupling between THz radiation and the CDW order parameter through resonant excitation of amplitude and phase modes that destabilize the commensurate David-star clusters across coherently coupled domains. The relaxation dynamics involve complex reorganization of the perturbed CDW state, wherein higher excitation powers populate metastable configurations characterized by topological defects such as phase slips and discommensurations. These defects effectively function as pinning centers that introduce significant energy barriers against recovery to the ground state. We have added the relevant description on the 13 page of the revised manuscript and incorporated this data into Fig. 2i.

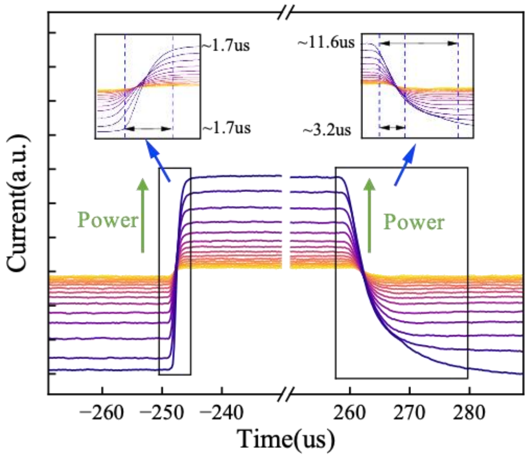

Revised Figure R7 **(Fig. 2i in the revised manuscript)** Expanded view of rise and fall edges in the temporal response with increasing power density.

REFEREE: 5) Are there any frequency dependencies for photocurrent signal under different incident optical powers?

AUTHORS' REPLY: 5) Thank you for your question. Following the referee's suggestion, to address the frequency dependence of the photocurrent under varying incident optical powers, we conducted additional experiments and present the results as follows. The results show that the frequency response remains the same across different power levels, suggesting it is mainly determined by the device's intrinsic properties rather than the incident power. However, we do observe that higher optical power increases the overall photocurrent magnitude, as expected. The additional data, now included in Fig.5, confirm this by showing overlapping frequency response trends at different power levels. We have updated the manuscript accordingly.

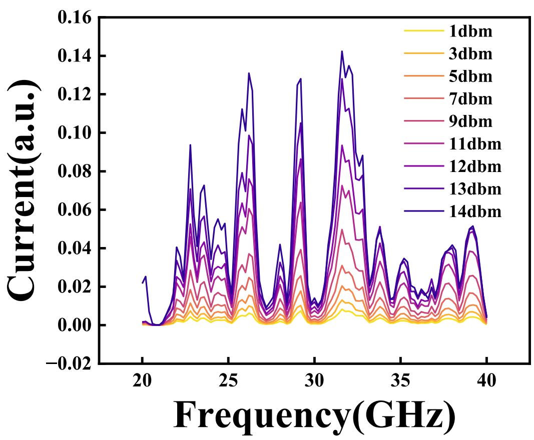

Revised Figure R8 **(Fig. 2i in the revised manuscript)** Frequency-dependent current response. The plot shows the normalized current output (a.u.) as a function of frequency (GHz) across the range of 20–40 GHz, demonstrating the device's photoresponse characteristics under varying incident excitation power.

REFEREE: 6) In caption of Fig. 2d "incident" appears two times.

AUTHORS' REPLY: 6) We appreciate the reviewer careful attention and helpful feedback on our manuscript. We have made revisions to the article accordingly.

REFEREE: 7) Why is the current responsivity under different bias voltages within the range of 0.24 THz to 0.3 THz? Is it related to the wavelength of CDW instability?

AUTHORS' REPLY: 7) Thank you for the reviewer's insightful question. **(1)** The THz waves in our experiment are generated by frequency multiplication of microwaves. Specifically, the range of 0.24–0.3 THz corresponds to the fundamental microwave frequencies of 26.7–33.3 GHz before passing through the frequency multiplier (VDI). **(2)** The frequency selection is influenced by the efficiency of the multiplier and the spectral distribution of the output power. The observed bias-dependent responsivity suggests that the detector operates in a regime where the applied electric field modulates the energy barrier between competing CDW phases. This tuning affects the nonlinear carrier transport and modifies the coupling efficiency between incident THz photons and the CDW-induced lattice distortions. Such bias-sensitive modulation is consistent with prior studies on CDW materials where external fields influence collective charge transport. Additionally, the butterfly-shaped antenna plays a crucial role in the observed frequency dependence. Its geometry determines the local field enhancement, leading to frequency-selective coupling that modifies the responsivity profile. The interplay between material-specific CDW dynamics and antenna-mediated field enhancement results in the measured response characteristics. We believe this combined effect accounts for the observed behavior within the 0.24–0.3 THz range.

REFEREE: 8) Are the changes induced from application of electric bias or incident THz pulses are reversible especially in the view of CDW instabilities? The validation of the truth table (Fig.3) should also be checked in multiple cycles and with a slight temperature change.

AUTHORS'REPLY: 8) We sincerely appreciate the reviewer's insightful questions regarding the reversibility of the electrically and optically induced phase transitions, as well as the stability of our logic operations. Regarding the reversibility of phase transitions and validation of the truth table, we have conducted extensive experiments on multiple 1T-TaS_2 devices to address both concerns (Figure S8 in Supporting Information). **(1)** As demonstrated in the newly provided experimental data (device 2-3), we have rigorously tested the reversibility of the phase transitions in multiple devices. In Device 2, we observe consistent switching behavior repeated over multiple cycles: Figure B shows the device undergoing two complete switching cycles with remarkable consistency. Under 4.1 mW/cm^2 THz illumination (red curves), the switching occurs at a lower electric field than in dark conditions (blue curves). Importantly, we observe a consistent shift of approximately 65 mV between the light and dark switching thresholds across both cycles. Figure C provides even stronger evidence of reversibility, showing four complete switching cycles under the same conditions. The threshold voltage difference between light and dark conditions remains stable at approximately 20 mV throughout all cycles, confirming the robust reproducibility of the electrically and optically induced phase transitions.

(2) The reviewer's concern regarding the validation of our truth table operations under repeated cycling is directly addressed by our new experimental data. Figure A shows the remarkable consistency of a third device (Device 1) over two complete switching cycles. Two additional important technical considerations further enhance the reliability of our measurements: First, our 1T-TaS_2 devices utilize flakes with thicknesses of approximately 40 nm. This thickness is significant as it places our devices in an optimal regime for observing the CDW phase transitions. As reported in ***Physical Review B 95, 121405(R) (2017)***, ultrathin TaS_2 samples do not exhibit phase transitions at low temperatures, while bulk samples readily do. Our 40 nm thickness ensures that the material maintains its rich phase diagram while benefiting from the enhanced controllability of reduced dimensions. Second, we have implemented a critical circuit design element by incorporating a 500 Ω series resistance in our measurement setup. This resistance serves as a current-limiting component that significantly reduces current fluctuations during switching events, leading to more stable and reproducible transitions. This approach minimizes Joule heating effects and prevents undesired drift in the device characteristics over multiple operational cycles.

Our investigations demonstrate that the NC-CDW and IC-CDW states exhibit full reversibility under electric bias and THz pulse stimuli, as documented in the revised Supplementary Figure S8. These transitions between the IC-CDW (low-resistance, 200 Ω) and NC-CDW (high-resistance, 500 Ω) states remain stable across multiple cycles with minimal hysteresis. This methodological refinement significantly enhances the reliability of our truth table operations (C → F, D → F, B → E), which are now governed solely by well-defined bias voltage thresholds (approximately 1.82 V as shown in the revised Figure 3b) and THz light intensity inputs. The updated experimental approach has been implemented consistently throughout the manuscript, including the revised Figures 3b and 3c at pages 17.

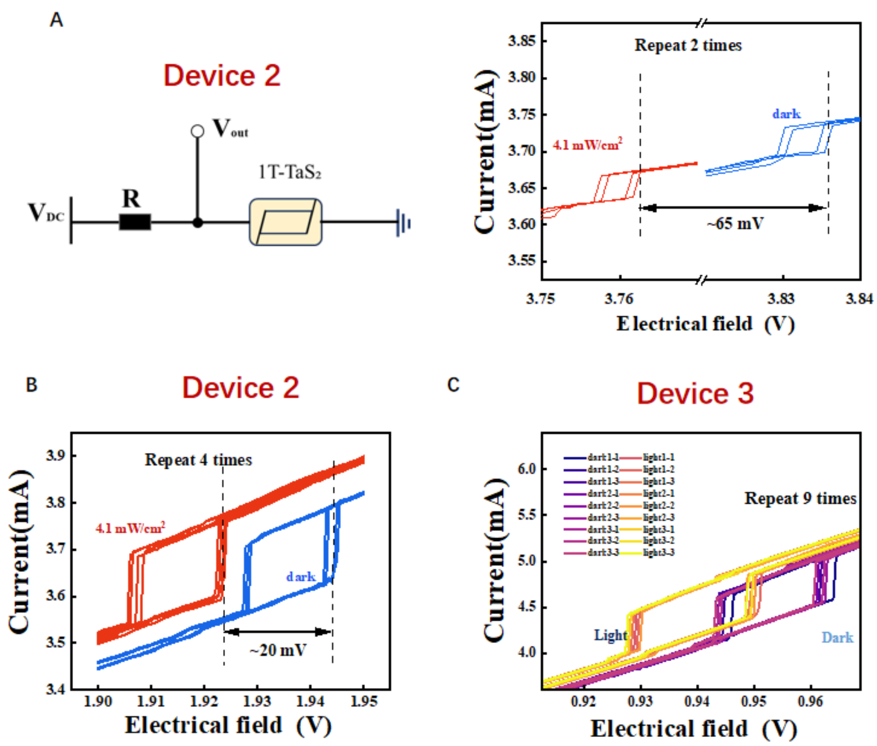

Revised Figure R9(Figure S8): (A) Measurement of device phase transition using series resistance. The phase change phenomenon can be altered by connecting resistors in series. Hysteresis IV curves under light and dark conditions with the 500Ω series resistance. (B) Hysteresis IV curves under light and dark conditions without the 500Ω series resistance. It was observed that the difference between the phase change voltage and the hysteresis voltage increased from 20mV to 65mV after connecting resistors in series. (C) Repetition of hysteresis IV curves.This process was repeated for three rounds, with each round consisting of three repetitions, verifying the reproducibility of the device's phase change hysteresis phenomenon.

REFEREE: 9) What is the optimal thickness of TaS2 for which it shows best THz optoelectronic sensing and reconfigurable logic computation? How does it vary with thickness?

AUTHORS' REPLY: 9) We sincerely appreciate the reviewer's insightful question regarding the optimal thickness of 1T-TaS_2 for THz optoelectronic sensing and reconfigurable logic applications. Based on our experiments, we find that a thickness range of approximately 40 nm provides an optimal balance, maximizing THz responsivity and resistance contrast while maintaining structural integrity and reproducibility in device fabrication.

Regarding the optimal thickness of 1T-TaS_2 for achieving the best THz optoelectronic sensing and reconfigurable logic computation, our study indicates that this is governed by a trade-off between performance and practical fabrication constraints. The photoelectric sensing and logic functionality we propose rely heavily on a large resistance contrast between the different charge-density wave (CDW) phases before and after the phase transition, which is more pronounced in thinner 1T-TaS_2 samples. However, there are critical limitations to consider as the thickness decreases. First, excessively thin samples, typically on the order of a few nanometers, exhibit a significant reduction in THz absorption due to diminished material volume, which compromises the optoelectronic response. Second, from a fabrication perspective, thinner 1T-TaS_2 layers are more susceptible to mechanical damage and defects during processing, such as exfoliation or device integration, leading to reduced yield and reliability under operational conditions.

REFEREE: 10) What is the role of hBN-TaS2 interface for propagation of CDW-transport properties especially in the vicinity of THz perturbing stimuli?

AUTHORS' REPLY: 10) We appreciate the reviewer's insightful question regarding the critical role of the hBN-TaS_2 interface in our device architecture. The hBN layer serves a protective role by preventing environmental degradation of TaS_2, such as oxidation or moisture-induced changes, which are known to compromise the long-term stability of 1T-TaS_2. Atomically smooth hBN encapsulation serves as an ideal dielectric environment that minimizes charge impurity scattering at the TaS_2 surface. The dielectric properties of hBN further enhance THz coupling efficiency by minimizing field attenuation, allowing the THz stimuli to effectively interact with the TaS_2 layer and modulate its CDW states. The hBN layers provide excellent thermal management during THz irradiation. When THz pulses interact with the 1T-TaS_2 flake, localized heating can occur, potentially introducing unwanted thermal effects.

Dear Editor,

We would like to express our gratitude to both the Editor and the reviewers for their valuable suggestions, which have significantly enhanced the scientific quality and readability of the manuscript. In response to the reviewers' comments, we have carefully revised the Response Letter. In accordance with the formatting guidelines for Nature Communications, we have further incorporated all modifications in the manuscript, with tracked changes highlighted in blue.

———REPLY TO REVIEWER 1———-

REFEREE: The authors have addressed all of my questions in their response. The manuscript now presents the results more clearly. If the novelty of this research is acknowledged by the other reviewers, I believe it would be appropriate for publication in Nature Communications.

AUTHORS' REPLY: We once again thank the reviewer for their professional comments, which will greatly help us improve the scientific quality of the manuscript.

———REPLY TO REVIEWER 2———-

REFEREE: 1) You mention that the response saturates beyond 0.25 V/um (0.7 V) and that higher voltages could induce irreversible changes or material damage. Could the authors clarify whether any hysteresis or degradation was observed when briefly exceeding this threshold during preliminary tests?

AUTHORS' REPLY: 2) We sincerely thank the reviewer for this important question regarding the long-term stability of our devices during repeated operations. To address this concern, we have conducted comprehensive repeatability tests across multiple devices to verify the reversibility and stability of the phase transitions. As shown in Figure S8, we performed multiple verifications tests that demonstrate remarkable consistency in device 2-3 performance within the safe operating range. Figure S8b illustrates that the device successfully completed two-four complete switching cycles with high consistency, while Figure S8c provides even stronger evidence of reversibility with nine complete switching cycles under identical conditions. The threshold voltage difference between light and dark conditions remains stable throughout all cycles, confirming that operation within the operation range does not induce cumulative structural or phase damage. Furthermore, we conducted additional experiments to identify the critical threshold beyond which permanent changes might occur. As shown in the provided Figure R2, when devices are subjected to bias voltages exceeding 3.3V, we observed a notable alteration in their phase transition voltages (shifting from 2940 mV to 2715 mV). Subsequent measurements revealed minor fluctuations in the phase transition point, accompanied by a subtle leftward shift.

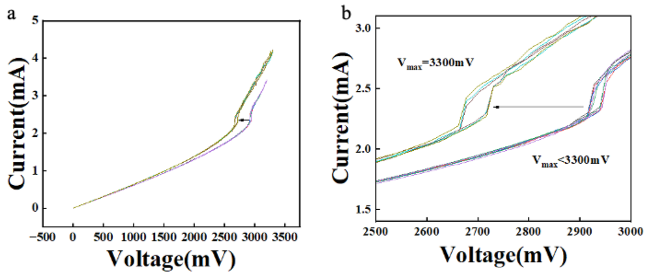

Figure R1 Hysteresis studies demonstrating phase transition reversibility and voltage threshold effects in 1T-TaS_2 devices.

REFEREE: 2) Is there experimental evidence (e.g., Raman, electrical cycling tests) confirming that operation within the 0-700 mV range avoids any cumulative structural or phase damage over repeated measurements?

AUTHORS' REPLY: 1) We sincerely appreciate the reviewer's insightful question regarding potential hysteresis or degradation when exceeding the voltage threshold. To address this concern, we've conducted extensive experiments on multiple 1T-TaS_2 devices to evaluate both the reversibility and stability of the electrically and optically induced phase transitions (Figure S8 in Supporting Information). Our experimental data from devices 3 demonstrates robust reversibility even after brief excursions beyond the typical operating threshold. Figure R1 provides even stronger evidence of reversibility, showing nine complete switching cycles under identical conditions. The threshold voltage difference between light and dark conditions remains stable at approximately 15 mV throughout all cycles, confirming the robust reproducibility of both electrically and optically induced phase transitions, even after brief excursions beyond the threshold.

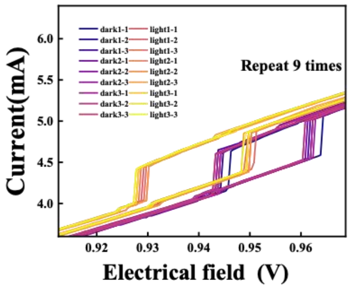

Revised Figure R2(Figure S8): Repetition of hysteresis IV curves.This process was repeated for three rounds, with each round consisting of three repetitions, verifying the reproducibility of the device's phase change hysteresis phenomenon.

REFEREE: 3)The reported resistance contrast between LRS (500 Ω) and HRS (200 Ω) results in a relatively modest switching ratio. Could the authors comment on whether this level of contrast is sufficient for robust logic operation, especially under noisy or low-signal conditions?

AUTHORS' REPLY: 3) Thank you for raising this important point regarding the resistance contrast in our terahertz optoelectronic logic system. While the reported resistance states (LRS: 500 Ω, HRS: 200 Ω) yield a relatively moderate switching ratio (~2.5), we emphasize that this figure must be interpreted within the context of the unique operational characteristics of CDW materials and the specific logic implementation architecture we have developed. Our device operates in the 0.3 THz regime with spectrally confined bandwidth ($\Delta f \approx 10$ GHz per channel), where the thermal noise floor is fundamentally governed by $P_{noise}=k_B T \Delta f$. Crucially, this represents a 100× noise reduction compared to conventional GHz-speed CMOS systems typically operating with $\Delta f \geq 100$ GHz bandwidths to achieve comparable data rates.

——— REPLY TO REVIEWER 3———

I am satisfied with the point by point response from the authors. The revised manuscript can be published with no further revision from my side.

AUTHORS' REPLY: We once again thank the reviewer for their professional comments, which will greatly help us improve the scientific quality of the manuscript.

- **We once again thank the editors and reviewers for their dedication.**

Dear Editor and the Reviewers,

We are pleased to submit the final revision of our manuscript, having now fully addressed all outstanding comments from Reviewer 2 in this round. Previously, we incorporated revisions for Reviewers 1 and 3 as outlined in our prior response. All three reviewers have now confirmed their satisfaction with the revisions and unanimously endorsed the manuscript's suitability for publication in ***Nature Communication***. We deeply appreciate the editors' and reviewers' insightful feedback, which has significantly strengthened the rigor and clarity of this work.

The first round:

————REPLY TO REVIEWER 1————-

REFEREE: The authors have addressed all of my questions in their response. The manuscript now presents the results more clearly. If the novelty of this research is acknowledged by the other reviewers, I believe it would be appropriate for publication in Nature Communications.

AUTHORS' REPLY: We once again thank the reviewer for their professional comments, which will greatly help us improve the scientific quality of the manuscript.

The second round:

————REPLY TO REVIEWER 2————-

REFEREE: The authors have satisfactorily addressed my concerns, and the manuscript now presents the results more clearly. Assuming the novelty of this research is acknowledged by the other reviewers, I support its publication in Nature Communications.

AUTHORS' REPLY: We once again thank the reviewer for their professional comments, which will greatly help us improve the scientific quality of the manuscript.

The first round:

————REPLY TO REVIEWER 3————-

I am satisfied with the point by point response from the authors. The revised manuscript can be published with no further revision from my side.

AUTHORS' REPLY: We once again thank the reviewer for their professional comments, which will greatly help us improve the scientific quality of the manuscript.

- **We once again thank the editors and reviewers for their dedication.**